J Supercond Nov Magn (2013) 26:2675–2678
DOI 10.1007/s10948-013-2158-8

ORIGINAL PAPER

Inhomogeneous Superconductivity in $BaPb_{1-x}Bi_xO_3$

P. Giraldo-Gallo · Hanoh Lee · M.R. Beasley · T.H. Geballe · I.R. Fisher

Received: 2 December 2012 / Accepted: 14 February 2013 / Published online: 15 March 2013

Abstract Transport and magnetization measurements of single crystas of $BaPb_{1-x}Bi_xO_3$, for Bi compositions spanning the superconducting phase diagram, show signatures of granular and inhomogeneous superconductivity, possibly associated with the nanoscale structural phase separation found for compositions around optimal doping. The material exhibits a field-tuned superconductor-to-insulator transition for Bi compositions $0.24 \leq x \leq 0.28$. For optimally doped samples ($x \approx 0.25$), the magnetoresistance curves show scaling, suggesting some kind of critical behavior.

Keywords Bismuthate superconductors · Superconductor-Insulator transition · Disorder · Percolation · Quantum phase transition · Structural phase separation

$BaPb_{1-x}Bi_xO_3$ is a solid solution of $BaPbO_3$, a low carrier density metal (10^{21} cm^{-3}); and $BaBiO_3$, a charge density wave (CDW) semiconductor comprising two distinct Bi sites [1]. Superconductivity in this material, with a maximum critical temperature of 11 K, arises for Bi compositions as low as $x = 0.05$, up to compositions below $x = 0.35$, where the gap associated with the CDW opens [2]. The type of pairing interaction giving rise to the CDW state, as well as superconductivity, is still a subject of debate. Models based on a negative-U mechanism [3] and on an enhanced electron-phonon interaction [4] have been proposed, the latter being supported by recent improved DFT band structure calculations [5]. Of special interest is the structural dimorphism (tetragonal and orthorhombic polymorphs) found for superconducting compositions by Climent-Pascual et al. in polycrystalline samples [6], and confirmed by Giraldo-Gallo et al. in single crystals [7]. The first study determined that the superconducting volume fraction scales with the relative proportion of the tetragonal phase, leading to the suggestion that only the tetragonal phase harbors superconductivity. The second study observed a nanometer-scale structural phase separation for optimally doped samples. The effect of the structural dimorphism, as well as the effect of chemical substitution, on shaping the phase diagram and in particular, the superconducting dome, are relevant questions not only to this family of bismuthate superconductors, but also in general to superconductivity of disordered systems and phase-separated materials [8–10].

In this paper, we present measurements of magnetic susceptibility and resistivity, as a function of temperature and magnetic field, of single-crystal samples of $BaPb_{1-x}Bi_xO_3$ for several superconducting compositions. These measurements augment our previously published results [7] and reveal the inhomogeneous nature of the material. We also present magnetoresistance measurements, which reveal evidence of a field-tuned superconductor-insulator transition with a temperature-independent crossing point for compositions close to optimal doping.

Single crystals of $BaPb_{1-x}Bi_xO_3$ with Bi compositions x between 0 and 0.35 were grown by slowly cooling a solution of $BaCO_3$, PbO, and Bi_2O_3. The bismuth concentration was determined by electron microprobe measurements, revealing a homogeneous composition (within the uncertainty of ± 0.02) within a sample as well as for different samples from the same batch.

P. Giraldo-Gallo (✉)
Geballe Laboratory for Advanced Materials and Department of Physics, Stanford University, Stanford, CA 94305, USA
e-mail: pgiraldo@stanford.edu

H. Lee · M.R. Beasley · T.H. Geballe · I.R. Fisher
Geballe Laboratory for Advanced Materials and Department of Applied Physics, Stanford University, Stanford, CA 94305, USA

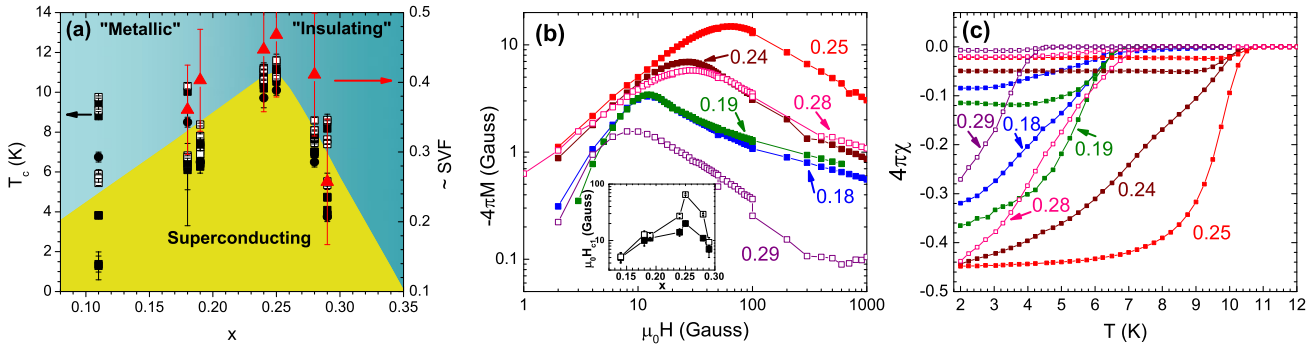

Fig. 1 (**a**) Variation of the critical temperature T_c (*left axis*) and estimation of the upper bound for the superconducting volume fraction (SVF) (*right axis*, *red triangles*) of single crystals of $BaPb_{1-x}Bi_xO_3$ as a function of the Bi concentration x. T_c values were obtained from measurements of resistivity (*open black squares* for a 90 % criteria, and *filled black squares* for a 50 % criteria) and magnetic susceptibility (*black filled circles*). (**b**) Zero-field-cooled magnetization vs. applied magnetic field at $T = 2$ K for Bi concentrations x of 0.18, 0.19, 0.24, 0.25, 0.28, and 0.29. The *inset* shows values of $H_{c1}(x)$ estimated from the peak magnetization (*open symbols*) and deviation from linear behavior (*solid symbols*). (**c**) Zero-field-cooled (*lower six curves*) and field-cooled (*upper six curves*) magnetic susceptibility measured by applying a field below H_{c1} ($H = 5$ Oe for samples with $x = 0.18$, 0.19, 0.24, 0.25, and 0.28; and $H = 3$ Oe for $x = 0.29$). (Color figure online)

Magnetization and DC magnetic susceptibility measurements were taken using a commercial Quantum Design SQUID magnetometer. For each composition, measurements were made for mosaics of approximately ten crystals, held in a gelatin capsule. Curves of magnetization vs. applied magnetic field for these samples, at a temperature of 2 K, are shown in Fig. 1(b). From these, approximate values of H_{c1} are obtained in two different ways. A crude estimate of H_{c1} can be obtained from the peak magnetization; this value slightly overestimating the field at which flux first penetrates the samples. Additionally, H_{c1} can be estimated from the field at which the magnetization curves deviate from a linear behavior, this value being closer to the field at which flux penetration starts. Values of H_{c1} determined in both manners show a clear compositional variation (inset to Fig. 1(b)), being largest for compositions near optimal doping ($x \approx 0.25$). Curves of field-cooled and zero-field-cooled magnetic susceptibility as a function of temperature are shown in Fig. 1(c). Data were taken using a field below $H_{c1}(x)$ for each of the compositions studied. An estimation of the upper bound to the superconducting volume fraction can be obtained from these measurements in two different ways: from the slope of the low field magnetization curves (for $H \ll H_{c1}$); and from the value of the zero-field-cooled magnetic susceptibility at 2 K, obtaining similar values from both methods. Demagnetization factors were not taken into account, which can only reduce the values obtained from the measurements, and are assumed to be independent of the Bi composition, given that the crystals for all compositions show similar morphologies. The average of this upper bound of the superconducting volume fraction obtained by both methods, as a function of Bi composition, is shown in Fig. 1(a) (right axis, red triangles), showing a maximum of 47 % for optimal doping ($x \approx 0.25$), and decreasing for lower and higher x values. This behavior is consistent with results previously found for polycrystalline samples [6], though with a reduced maximum volume fraction, possibly due to the different conditions and cooling rates used to grow single-crystal samples.

Resistivity measurements were obtained using a four probe technique. Electrical contact was made by evaporating gold pads on the top face of the crystals and attaching gold wires with silver epoxy. As a result of the irregular shape of the cleaved crystals, given the highly 3D crystal structure of this material, a large uncertainty in the geometrical factor needed to calculate the resistivity from these resistance measurements is introduced. In order to minimize this uncertainty, five samples of each composition were measured, and the room temperature resistivities, calculated with the individual geometrical factors, were averaged in order to scale the resistivity of a representative sample of each batch. The resulting curves are shown in Fig. 2(a), for compositions ranging from $x = 0$ (metallic parent compound) up to $x = 0.29$ (near the boundary of the CDW transition). Low Bi concentrations show "metallic-like" behavior, with a positive temperature coefficient, whereas compositions above $x = 0.24$ show "insulating-like" behavior, with a negative temperature coefficient (but not an activated temperature dependence). The turning point between insulating and metallic behavior appears to occur very close to optimal doping and before the composition where the gap associated with the CDW opens ($x \approx 0.35$). Nevertheless, sample-to-sample variation in both the temperature dependence of the resistivity and superconducting transition temperatures for samples with the same nominal Bi composition is evident and reveals the inhomogeneous nature of this material. Normalized resistivity curves for five different samples of compositions below, at, and above optimal doping are shown in Fig. 2(b),

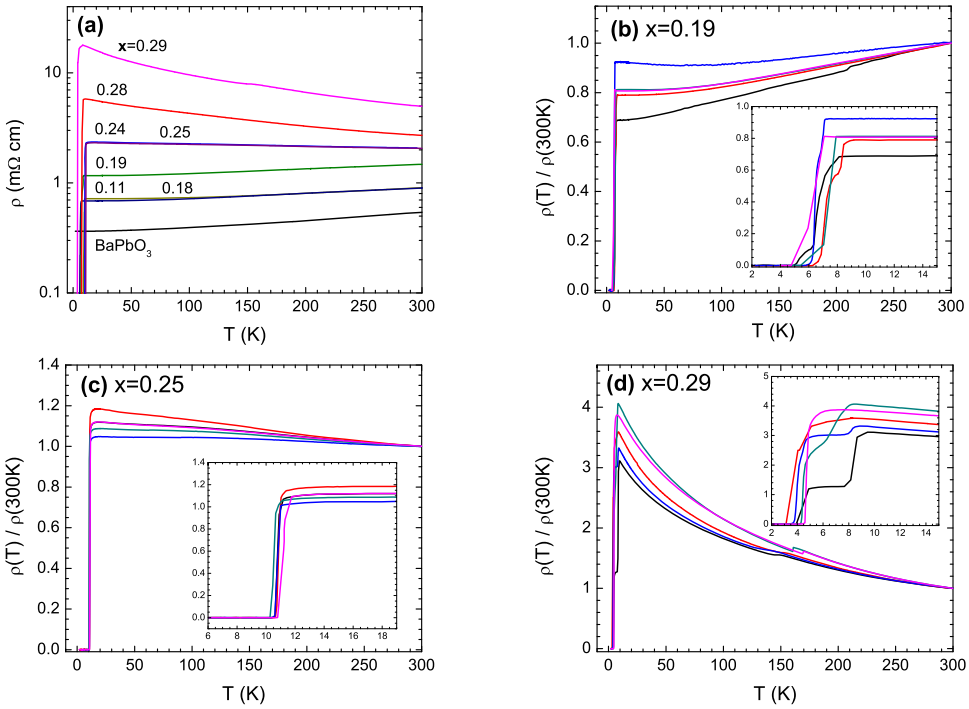

Fig. 2 (**a**) Temperature dependence of the absolute value of the resistivity for representative samples of $BaPb_{1-x}Bi_xO_3$ with Bi composition x spanning the superconducting phase diagram. (**b**)–(**d**) Normalized resistivity $\rho(T)/\rho(300\ \mathrm{K})$ as a function of temperature for five different samples from the same batch, with bismuth concentration of (**b**) $x = 0.19$, (**c**) $x = 0.25$, and (**d**) $x = 0.29$. (Color figure online)

2(c), and 2(d), respectively. Samples around optimal doping show the least variation both in the temperature dependence of the normal-state resistivity and in T_c. For compositions below and above optimal doping, the superconducting transition for all samples is quite broad, and often exhibits double-stepped transitions. The dispersion in the superconducting transition, both due to sample-to-sample variation and to the width of the transition for each sample, is summarized in the phase diagram in Fig. 1(a), where T_c obtained from resistivity measurements has been determined by two criteria: 90 % and 50 % drop on the normal state resistivity, calculated from a low temperature fit before superconducting contributions to the resistivity appear. Error bars in each quantity represent standard deviations from measurements of at least five samples.

Magnetoresistance measurements for different temperatures below T_c, for three representative Bi compositions spanning the phase diagram, are shown if Fig. 3. The different isotherms were symmetrized from positive and negative magnetic field sweeps up to 14 T. "Metallic-like" compositions ($x < 0.24$) show zero magnetoresistance for fields above H_{c2}, and the superconducting transition is homogeneously suppressed as expected. However, samples at optimal doping and above ($x \geq 0.24$) show a qualitative different behavior, with the characteristics of a superconductor-insulator transition. Figure 3(b) and 3(c) display data for representative samples for two of these compositions. For low magnetic fields, they exhibit a "superconducting-like" behavior (decreasing resistivity with decreasing temperature), whereas for high magnetic field, the behavior is "insulating-like" (increasing resistivity with decreasing temperature). The separatrix between these two regimes has different characteristics for different bismuth compositions. For optimally doped samples ($x = 0.24$ and 0.25), this separatrix is demarcated by a temperature-independent crossing field, H_c, for a wide temperature range that goes from approximately 8 K, down to the lowest temperature measured (2 K) for some samples, and to 3 K or 4 K for most of the samples measured [7]. For higher values of bismuth concentrations ($x = 0.28$ and 0.29), the transition from superconductor to insulator is not characterized by a temperature independent crossing point at any temperature range (down to 1.5 K). Furthermore, quite remarkably, over the whole range of temperatures where the crossing field is temperature-independent, the magnetoresistance curves appear to exhibit scaling of the form $\rho(T, H) = \rho_c F(|H - H_c|T^{-1/z\nu})$ as can be seen in the inset to Fig. 3(b), suggestive of critical behavior. Values of the critical exponents $z\nu$ were calculated by an iterative method for several samples around the optimal composition, obtaining an average value of $z\nu = 0.69 \pm 0.03$ [7].

The phenomenology described above, together with the broad and inhomogeneous superconducting transitions as seen in resistivity; superconducting volume fractions of less than 50 % as determined by magnetization and magnetic susceptibility measurements; and the observed polymorphic nature with nanometer-scale structural variations as reported in [7] suggest a scenario where the effects seen in granular

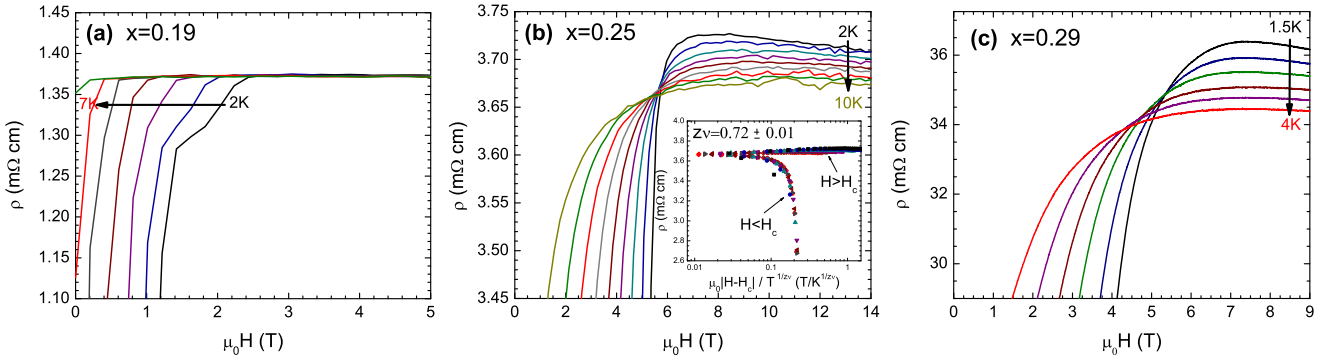

Fig. 3 Isotherms of resistivity vs. magnetic field for bismuth concentrations of (**a**) $x = 0.19$ (2 K to 8 K in 1 K steps), (**b**) $x = 0.25$ (2 K to 10 K in 1 K steps), (**c**) $x = 0.29$ (1.5 K to 4 K in 0.5 K steps). For the nearly optimally doped compositions $x = 0.24$ and 0.25, a temperature-independent crossing point is evident for temperatures below approximately 8 K. The *inset to panel* (**b**) shows the scaling analysis of the magnetoresistance curves for the $x = 0.25$ sample (ρ vs. $|H - H_c|/T^{1/z\nu}$), using the value of $z\nu$ that minimizes the dispersion of the points ($z\nu = 0.72 \pm 0.01$ for this particular sample). (Color figure online)

superconductors are playing an important role in determining the superconducting properties in this material, particularly if one of the structural polymorphs (tetragonal and orthorhombic) is non-superconducting (orthorhombic), as has been claimed by several authors [6, 11, 12], or even if the tetragonal and orthorhombic polymorphs have different T_c's [13, 14]. The granular nature of this problem suggest two initial avenues for understanding the experimental results, based first on a classical effective medium theory [15], and second on a field-tuned quantum phase transition [16]. As presented in a previous paper [7], neither of these frameworks describe in a satisfactory fashion the observed phenomenology. The classical effective medium theory requires an unphysical level of fine tuning in order to obtain an apparent temperature independent crossing point over a certain temperature range. On the other hand, the field-tuned QPT reproduces the phenomenology seen at optimal doping only if the effective dimensionality of the system is assumed to be 2D, which seems unlikely given that our measurements are of bulk, 3-dimensional single crystals. Although high resolution transmission electron microscopy (HRTEM) measurements show features that are suggestive of a preferred orientation of the polymorph intergrowths [7], which could give rise to some kind of "hidden 2-dimensionality," further analysis is required in order to determine whether such a scenario is feasible. It remains to be seen whether a full theoretical treatment including aspects of both percolation and quantum-critical scaling can satisfactorily reproduce and reconcile the transport phenomenology and the microstructure features observed for samples across the superconducting dome.

Acknowledgements The authors thank R. Jones for help with microprobe measurements, and S.A. Kivelson, A. Kapitulnik, and N.P. Breznay for helpful discussions. This work is supported by AFOSR Grant No. FA9550-09-1-0583.

References

1. Uchida, S., Kitazawa, K., Tanaka, S.: Phase Transit. **8**, 95 (1987)
2. Tajima, S., et al.: Phys. Rev. B **32**, 6302 (1985)
3. Taraphder, A., et al.: Phys. Rev. B **52**, 1368 (1995)
4. Meregalli, V., Savrasov, S.Y.: Phys. Rev. B **57**, 14453 (1998)
5. Yin, Z.P., Kutepov, A., Kotliar, G.: e-print arXiv:1110.5751v1 (2011)
6. Climent-Pascual, E., Ni, N., Jia, S., Huang, Q., Cava, R.J.: Phys. Rev. B **83**, 174512 (2011)
7. Giraldo-Gallo, P., Lee, H., Zhang, Y., Kramer, M.J., Beasley, M.R., Geballe, T.H., Fisher, I.R.: Phys. Rev. B **85**, 174503 (2012)
8. Steiner, M.A., Breznay, N.P., Kapitulnik, A.: Phys. Rev. B **77**, 212501 (2008)
9. Jorgensen, J.D., et al.: Phys. Rev. B **38**, 11337 (1988)
10. Fratini, M., Poccia, N., Ricci, A., Campi, G., Burghammer, M., Aeppli, G., Bianconi, A.: Nature **466**, 841 (2010)
11. Sleight, A.W., Cox, D.E.: Solid State Commun. **58**, 347 (1986)
12. Marx, D.T., et al.: Phys. Rev. B **46**, 1144 (1992)
13. Oda, M., Hadika, Y., Katsui, A., Murakami, T.: Solid State Commun. **60**, 897 (1986)
14. Asano, H., et al.: Jpn. J. Appl. Phys. **27**, 1638 (1988)
15. Landauer, R.: AIP Conf. Proc. **40**, 2 (1978)
16. Fisher, M.P.A.: Phys. Rev. Lett. **65**, 923 (1990)